ON THE IMPACT OF ANEMOMETER SIZE ON THE VELOCITY FIELD IN A CLOSED WIND TUNNEL

I. CARE[(1)] and M. ARENAS[(2)]
(1): LNE- CETIAT, isabelle.care@cetiat.fr
(2): EDF R&D, mario.arenas@edf.fr

Abstract

In the present paper, experimental and numerical investigations of the flow around different types and sizes of anemometers are presented and discussed.
The measurements of the flow field at different distances upstream to the anemometer are performed with a laser Doppler Anemometer. The computational results are in rather good agreement with the experimental ones and show that anemometers may induce a strong distortion of the velocity field, even far upstream the anemometer.

1. Introduction

The effects of the distortions of the velocity field by a body introduced in a wind tunnel are even now not fully explained. Some investigations have already been led, mainly related to aeronautical research [1, 2] and wind energy [3]. In these cases, wind tunnels are used as experimental tool to help in the design of aircraft or wind turbines parts. However, because of its finite size, the flow conditions are slightly different in a wind tunnel compared to those in an unbounded flow field where the bodies under test are used. Empirical equations are established to correct the effects of buoyancy, solid and wake blockages on the results.
In industrial field, anemometers are more and more often used to measure a flow rate in ducts for efficiency and/or safety related subjects. Industrial needs are now to have reliable and accurate measurements. This involves taking into account the effect of anemometer intrusion in the duct during the measurement process as well as improving the calibration methods of anemometers in wind tunnels.
Comparisons between National Metrology Institutes or calibration laboratories are good tools to demonstrate if the intrusion effect of the anemometers is taken into account in a suitable way. H. Mueller [4] has shown for example in EURAMET 827 comparison that the deviations between the National Metrology Institutes which may be observed could be due to the transfer standard itself and more specifically to the interaction between them and the wind tunnel where the calibration is performed.
As a contribution to the understanding of the phenomenon, EDF R&D and LNE-CETIAT have led together a study to evaluate the impact of an anemometer on the velocity field in a wind tunnel. Experimental measurements in a closed wind tunnel and numerical simulations have been performed simultaneously, for different types and sizes of anemometers (from Pitot tube to large vane anemometer).
The interest of the simultaneous experimental and numerical investigation is the possibility to validate directly the numerical results by the mean of the experimental ones. Once the numerical model has been validated, numerical experiments are easier to run than experimental ones to investigate further the blockage effect of anemometers when geometrical parameters are varying.

2. Experimental set-up

Experimental investigations are carried out in a closed wind tunnel. The objectives are to highlight the disturbing effect of the anemometer on a velocity field and to record experimental data to validate the numerical investigations.

2.1. The experimental set-up

The tests are performed in a closed wind tunnel used for the calibration of anemometers at LNE-CETIAT. The test section is rectangular. The top and bottom walls are parallel and the side walls diverge slightly from the inlet to the outlet of the test section. This feature reduces the effect of the increase of the boundary layer between the inlet and the outlet of the test section.

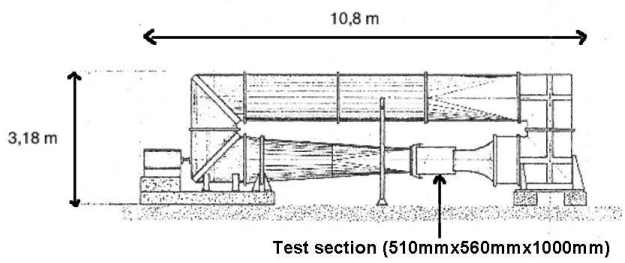

Fig. 1 - Closed wind tunnel at LNE-CETIAT used for the experimental investigations

The wind tunnel is characterized by a velocity field homogeneous in space and stable in time. Anyway, these characteristics are quantified and taken into account in the uncertainty budget. The axial velocity measurements are performed with a 1D Laser Doppler Anemometer. Its measurement uncertainty is the smallest one which can be reached by an anemometer. The usual uncertainty is around 0.5% of the measured value. The non-intrusive characteristic insures that the velocity field distortion is only due to the anemometer under test.
Four different types of anemometers are investigated: On Fig. 2. below, from left to right:

- A Pitot tube designed according ISO 3966 [5]
- a thermal anemometer
- a small size vane anemometer (14 mm diameter)
- a large size vane anemometer (100 mm diameter)

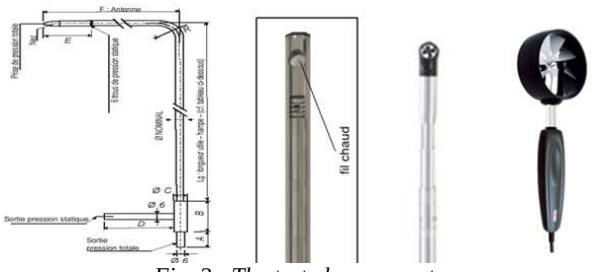

Fig. 2 - The tested anemometers

These anemometers have been chosen as representative of the ones which can be used in the industrial area: from the Pitot tube, the less intrusive to the 100 mm vane anemometer, the more intrusive.
The experimental program is the same for all the anemometers. The tests have been performed at 2, 5 and 18 m/s. These velocities have been selected according to the measuring range of the anemometers.
Axial Velocity fields have been characterized in 3 surface planes upstream the anemometer: at 20 mm, 100 mm and 300 mm which gives approximately 3000 measurement points.

2.2. Results

To visualize and analyze the measurements results, velocity profiles and fields have been drawn.
Whatever the velocity is, the velocity distributions are the same around the anemometers. Fig. 3 displays a comparison of the axial velocity fields at 20 mm and 300 mm upstream the different anemometers.

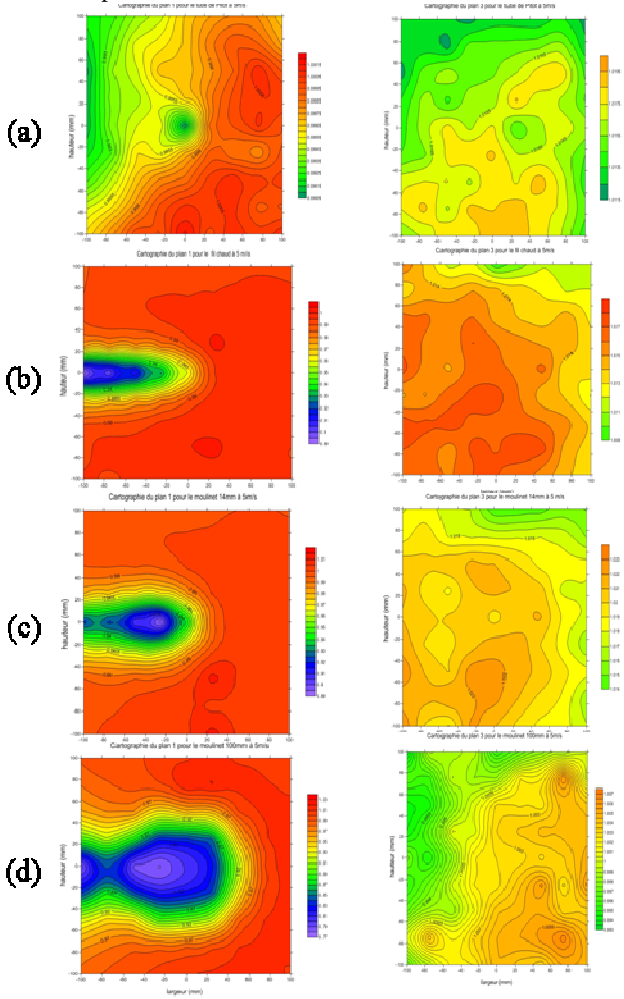

Fig. 3 -Axial velocity fields at 20 mm upstream (left) and 300 mm (right) upstream (a) Pitot tube, (b) thermal anemometer, (c) 14 mm vane anemometer, (d) 100 mm vane anemometer

At 20 mm, the signature of the anemometer is clearly seen, even for the Pitot tube, the less intrusive one. The disturbances are not only due to the sensor itself but also to the support which can be very prominent (Fig. 3 (d) left) in the more recent design of instruments. It means that, when thinking about an obstruction coefficient of anemometers in a closed circuit, the support mustn't be forgotten.
At 300 mm upstream, there is almost no more track of the anemometer, except for the larger one (Fig. 3 (d) right). In the used wind tunnel, this distance seems to be large enough to recover a free flow in the case of usual anemometers. A similar characterization should be conducted for other duct's sizes.
To quantify the impact of the anemometer Fig. 4 shows the weighted central velocity with respect to the velocity at 300 mm.

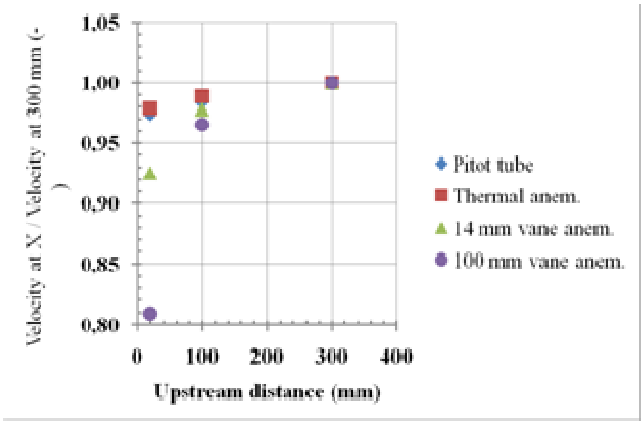

Fig. 4 - Central velocity variation upstream the anemometers

The figure above shows clearly that the velocity measurement is strongly affected by the presence of the anemometer in the flow.
In the case of a calibration in a closed wind tunnel with a procedure of simultaneous readings of the both anemometers, it becomes obvious that the distance between the reference anemometer and the instrument under test should be large enough to minimize the impact of this flow distortion.
In the case of industrial measurements, the presence of the anemometer in the duct should also be taken into account to correct the velocity measurement since the aim is to know what the velocity would be without the anemometer.
These experimental results should be considered as preliminary ones to define how to improve the blockage effects correction for the National Metrology Institutes.
To explore more test configurations, numerical simulation is a good tool and these experimental results can also be considered as an important database for validation.

3. Numerical investigation

Code_saturne© 2.0 was used for the numerical investigation. It is an open source computational fluid dynamics tool developed by the French electricity producer EDF. Code_saturne© is a Navier-Stokes equations solver. It can be used in a large range of applications, including steady or unsteady, laminar or turbulent, isothermal or not, incompressible or weakly dilatable flows, in 2D, 2D-axisymmetric and 3D cases. Scalar transport is also possible.

It includes several turbulence models, such as the so-called Reynolds-Averaged or the Large-Eddy Simulation ones. In addition, it deals with several specific physical models.
Code_Saturne© is based on a co-located Finite Volume approach, that accepts meshes composed by cells of any type (tetrahedrons, hexahedrons, prisms, pyramids, polyhedrons, ...) and grid structures of any type (unstructured, block structured, hybrid, conforming or with hanging nodes, ...).
EnSight software has been used for the post processing and visualization.

3.1. Meshing, boundary conditions, turbulence model and CFD code

The first step of the numerical investigation is the creation of a realistic grid. A hexahedral multi-block grid was created for each anemometer. Quality mesh criterion (skewness, smoothness and aspect ratio) have been checked out and a refined mesh near the walls has been chosen to guarantee a high quality mesh. Particular details about grids will be only presented for Pitot tube and large size vane anemometer. However results will be presented for all anemometers as for experimental study.

3.1.1. Pitot tube and vane anemometer grids

The grid presented in Fig. 5 corresponds to a segment of the CETIAT's wind tunnel (1.15m length). The grid consists of an inlet, a Pitot tube (or a vane anemometer) and an outlet. Anemometers as well as top, bottom and sides faces are set to walls. Anemometers are placed in a horizontal plane of the CFD-domain, the cross-sectional area is uniform and measures 560 mm wide by 510 mm high. Mesh is composed of 2.5M cells for the Pitot tube and 3.4M cells for the vane anemometer.

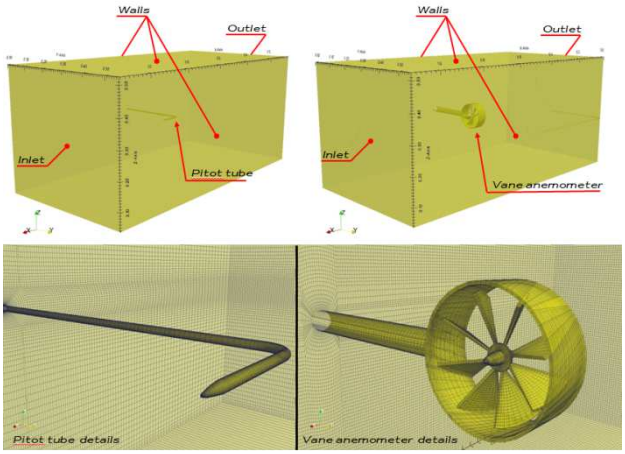

Fig. 5 - Modeled geometry (Pitot tube and vane anemometer)

3.1.2. Boundary conditions

The boundary conditions are stated as follows:
At inlet, a value of the mass flow rate 0.659 kg/s (for 2 m/s), 1.646 kg/s (for 5 m/s) and 5.927 kg/s (for 18 m/s) is prescribed while, at exit, an output flux is fixed.
All the walls are defined as adiabatic and with free slip.
The reference pressure and temperature are set to 1 atm and 25 °C.

Regarding turbulence model, it was chosen a first-order two equations model k-ε with linear production and a second-order Reynolds stress transport model Rij-ε SSG (Speziale, Sarkar and Gatski). First results have shown the k-ε model has got a good behaviour in the zone of interest (upstream the anemometer). The k-ε model seems to be a good compromise between representativeness and time consumption. Nevertheless if the zone of interest was different (downstream zone for example), a Rij-ε SSG model would be strongly recommended.

In order to guarantee stability of calculations, an appropriate time step has been chosen for each anemometer and inlet velocity, see Table 1 below. Time step has been calculated for a CFL (Courant Friedrichs Lewy) number near to 1. Convergence was verified by monitoring critical points of the CFD-domain.

Table 1. Numerical settings

Anemometer	Time step (s)			Number of iterations		
	2m/s	5m/s	18m/s	2m/s	5m/s	18m/s
Pitot tube	1×10^{-04}	1×10^{-04}	1×10^{-05}	4000	3000	3500
Vane anemometer	9×10^{-05}	4×10^{-05}	1×10^{-05}	6500	6500	6500

3.2. Means hypothesis (Geometry simplifications)

A number of geometrical simplifications were made during grids creation phase. First, cross-sectional area of the CETIAT's wind tunnel is not uniform unlike the uniform section chosen for modelling it. It could have an impact on the velocity profile as will be explained below.
The exact geometry of the Pitot tube was modelled save for the pressure holes (static or total).
For thermal anemometer only the very fine wire wasn't modelled. Regarding the 14 mm vane anemometer the main simplifications were the blades that couldn't be modelled for saving a reasonable number of cells.
Finally the handle of the 100 mm vane anemometer was modelled by a uniform cross section cylinder and blades are fixed.

3.3. Results and discussion

Computational fluid dynamics was used to calculate the velocity fields in the wind tunnel for different anemometers. Fig. 6 shows the velocity fields at 20 mm and 300 mm upstream for the different anemometers. Analysing velocity isolines it seems smoothed compared to experimental velocity fields (Figure 3) but the structure is quite similar.

As it was stated earlier, the print of each anemometer is easily distinguished in the 20 mm plane, even for the Pitot tube, contrary to 300 mm plane where fields seem to be no more disturbed. When examining in detail the speed deviation at 20 mm plane, only Pitot tube has got a relatively minor deviation between minimal and maximal speed (less than 1%). Regarding the others, speed deviation is 8 % for thermal anemometer and can reach 11% and 15 % for 14 mm vane anemometer and 100 mm vane anemometer.

(a)

(b)

(c)

(d)

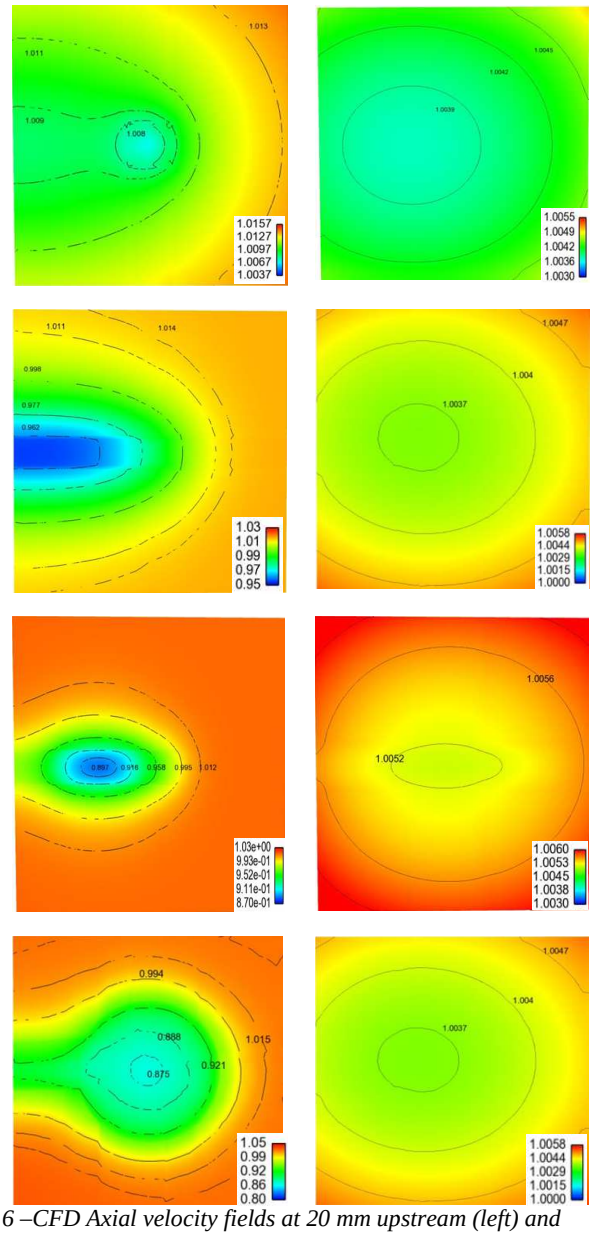

Fig. 6 –CFD Axial velocity fields at 20 mm upstream (left) and 300 mm (right) upstream (a) Pitot tube, (b) thermal anemometer, (c) 14 mm vane anemometer, (d) 100 mm vane anemometer

To quantify the calculated impact of the anemometer on the flow field as for the experimental results (cf Fig. 4), the weighted central velocity with respect to the velocity at 300 mm is presented in Fig. 7.

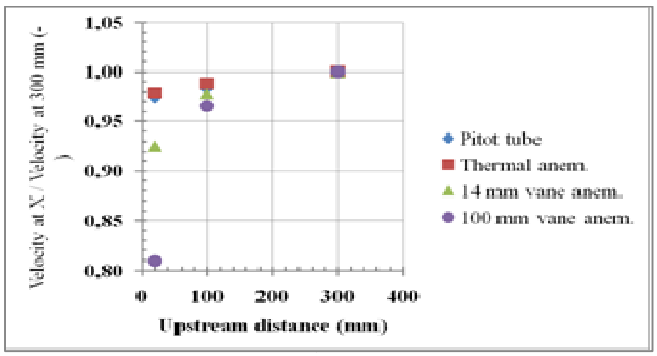

Fig. 7 - Central velocity variation upstream the anemometers from CFD results

The experimental observed perturbation of the velocity is confirmed particularly for the large size vane anemometer where velocity decreases to 85% of its value at 20 mm plane.

4. Comparison between experimental and numerical results

4.1. Boundary layer correction

Numerical results presented above are very close to experimental ones. From a qualitative point of view the same conclusions can be made from experimental or numerical study. Both of them show which anemometer has the biggest impact on velocity perturbation and also from which distance upstream the velocity field seems to be undisturbed by the anemometer. From a quantitative point of view, deviation between numerical and experimental results exists and could be explained by geometric simplifications and uncertainties of CFD. Uncertainty quantification in CFD wasn't part of this study and anemometers were modeled as far as possible. One of the more important geometric simplifications was the uniform cross-sectional area of the wind tunnel. Fig. 8 (blue line) shows the axial velocity profile for the Pitot tube. Save for the closest segment from the Pitot tube ($x < 0.1$ m), the trend curve is negative. Velocity increases when approaching Pitot tube on the contrary of experimental data where velocity decreases when approaching Pitot tube. Analysing differences, the simplifications of the variable cross-sectional of the wind tunnel seems to be the reason of this discrepancy. When the walls are parallel, from the inlet of the wind tunnel, the boundary layer increases and the effective section of the tunnel decreases. As a consequence, the central velocity increases. This phenomenon is observed in the simulated results. The vertical walls in which the experimental tests have been performed are slightly diverging. The reason of this particular design could be to counterbalance the growth of the boundary layer.

Taking into account the results of the CFD, the boundary layer theory and the geometry of the wind tunnel, a correction is applied to the numerical results

The faces of the wind tunnel have been designed to make up for the effects of the boundary layer. Characterization of the numerical boundary layer allowed quantifying the evolution of it. $\delta(x)$, then velocity can be corrected by the same factor. Fig. 8 (red line) shows the corrected velocity profile. Experimental and CFD results can be compared now.

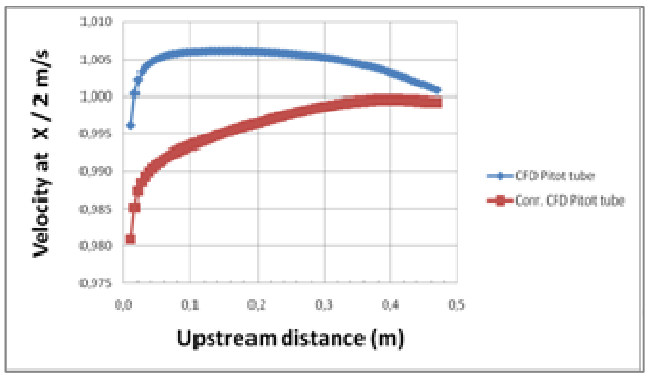

Fig. 8 –Axial velocity profile for Pitot tube

4.2. Axial velocity profiles: CFD Vs. Experimental data

To evaluate the impact of the anemometers on the flow field and compare experimental results and CFD calculations, the deviation between the central axial velocity at 20 mm and the one at 300 mm upstream the anemometer is presented for each anemometer and each velocity in Fig. 9 below.

(a)

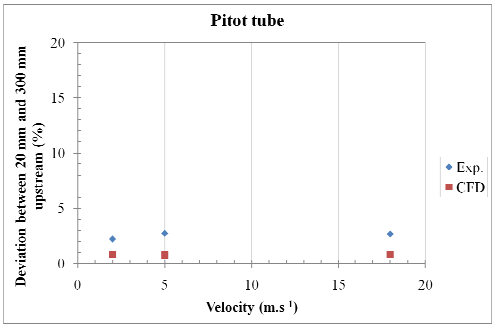

(b)

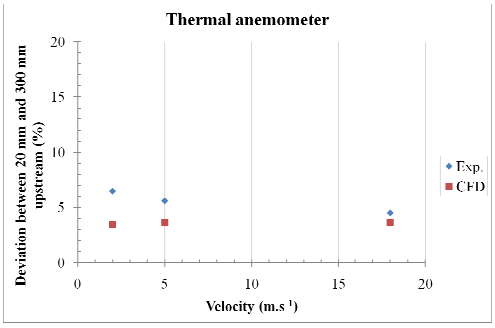

(c)

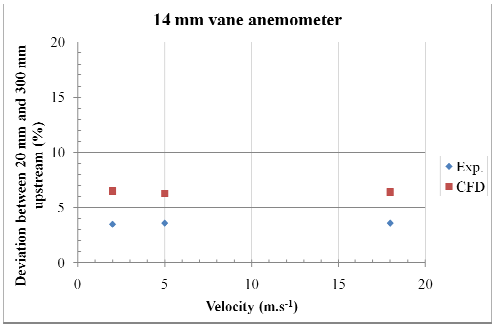

(d)

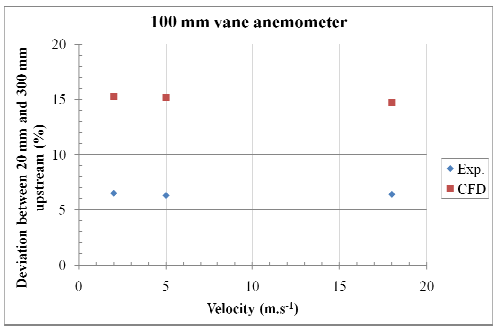

Fig. 9 –Deviation between central axial velocity at 20 mm and 300 mm upstream: Exp. Vs. CFD. (a) Pitot tube, (b) thermal anemometer, (c) 14 mm vane anemometer, (d) 100 mm vane anemometer

Whatever the velocity is, the behavior is the same. Except for the 100 mm vane anemometer, the comparison between experimental results and computational ones is rather satisfactory. This large size anemometer is the one for which the geometrical simplifications are the biggest. This could explain this behavior.

5. Conclusions and future work

The impact of 4 anemometers has been studied by an experimental and numerical approach and a rather good agreement was found between experimental and numerical results. The distortion of velocity field can be important for some anemometers (deviation of 20% for the biggest one).

It has been seen that the upstream effect of anemometer can be very important even far upstream. In the case of a calibration procedure, this minimum distance which depends on the wind tunnel characteristics must be taken into account to place the anemometer under test and the reference one.

In the case of velocity measurements in duct, the obstruction effect of the anemometer has to be taken into account as well to correct the velocity measurement. It is therefore important to know what the correction to apply could be. Considering the obstruction coefficient of anemometers calculated as the ratio of the section hidden by the anemometer over the section of the wind tunnel, Fig. 10 presents for the different tested anemometers the mean deviation of Fig. 9 vs the obstruction coefficient.

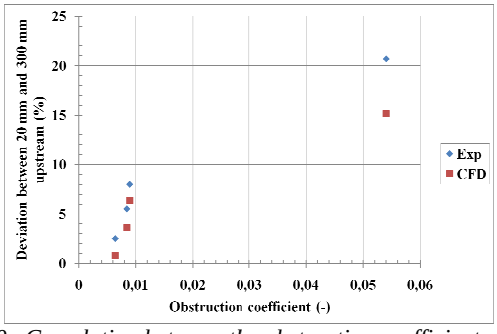

Fig. 10 –Correlation between the obstruction coefficient and the velocity deviation

The numerical experiments could be considered as a preliminary phase for the study of the blockage effect of anemometers in a wind tunnel to complete the former curve and try to find a relationship between obstruction

coefficient and correction to apply. Indeed, numerical experiments can be led more easily than experimental ones when changing geometrical parameters such as dimensions or even shape of the wind tunnel to cover a wider range of obstruction coefficient.

References

[1] – E.C. Maskell, "A theory of the blockage effects on bluff bodies and stalled wings in a closed wind tunnel", Aeronautical Research Council, Reports and Memoranda, N°3400, November 1963

[2] – R.W.F. Gould, "Wake blockage corrections in a closed wind tunnel for one or two wall-mounted models subject to separated flow", Aeronautical Research Council, Reports and Memoranda, N°3649, February 1969

[3] – T.Y. Chen, L.R. Liou, "Blockage corrections in wind tunnel tests of small horizontal-axis wind turbines", Experimental Thermal and Fluid Science, vol. 35, pp 565-569, 2011

[4] – H. Mueller, "Final Report, LDA-based intercomparison of anemometers, EURAMET Project n°827", EURAMET and BIPM databases

[5] – "Measurement of fluid flow in closed conduits. Velocity area method for regular flows using Pitot static tubes", ISO 3966, 2008

[6] – Code_saturne©: EDF's general purpose computational fluid dynamics (CFD), http://research.edf.com